MARMARA UNIVERSITY

FACULTY OF ENGINEERING

A METHODOLOGY FOR PUMP-AS-TURBINE SYSTEM IN A REAL LIFE ENERGY RECOVERY APPLICATION

Ahmet Yüksel TOPRAK, Furkan Nazmi ŞİT

GRADUATION PROJECT REPORT

Department of Mechanical Engineering

SUPERVISOR

Prof.Dr. Emre ALPMAN

ISTANBUL, 2022

MARMARA UNIVERSITY

FACULTY OF ENGINEERING

A Methodology for Pump-as-Turbine System in a Real Life

Energy Recovery Application

by

Ahmet Yüksel TOPRAK, Furkan Nazmi ŞİT

July 15, 2022, Istanbul

SUBMITED TO THE DEPARTMENT OF MECHANICAL ENGINEERING IN PARTIAL FULFILLMENT OF THE REQUIREMENTS FOR THE DEGREE

OF

BACHELOR OF SCIENCE

AT

MARMARA UNIVERSITY

Signature of Author(s) .....

Department of Mechanical Engineering

Certified By .....

Project Supervisor, Department of Mechanical Engineering

Accepted By.....

Head of the Department of Mechanical Engineering

ACKNOWLEDGEMENT

First and foremost, we would like to express our thankfulness to our supervisor Prof. Dr. Emre ALPMAN for the valuable guidance and advice on preparing this thesis and for giving us moral and material support. We would like to thank all the people who contributed to the digital library of Marmara University, which enabled us to conduct such an extensive literature review within the scope of the project.

June, 2022 **Ahmet Yüksel TOPRAK, Furkan Nazmi ŞİT**

CONTENTS

ABSTRACT

Small hydro-power projects getting popular around the world by presenting low initial and maintenance cost. Although, small hydro-projects have a lot of application areas, the best way to use them is applying in WDNs. Because, in WDNs, PRVs are used to reduce pressure which is outgoing to towns or urbans, to protect pipelines and failures on buildings. While reducing the pressure with PRVs, energy is lost, but if we use a centrifugal pump instead of a PRV, we can regenerate some of that lost energy. The main purpose of using centrifugal pump instead of a turbine is lower costs. Also, turbine needs to be designed specially to the area, but pumps are ready to use as a Pump as Turbine (PAT). Selection, installation and control strategy of a PAT in a WDN must consider accomplishing pressure reduction and flow rate demand. In this work, we describe a methodology for selection of the most suitable PAT and best control criteria for a WDN. Then, knowing the performance and efficiency curves of the pump, it is possible to estimate curves of the turbine mode by using 1-D Performance Prediction Model.

SYMBOLS

$\boldsymbol{H}$: Site Head Characteristic $[m]$

$\boldsymbol{Q}$: Site Flow Characteristic $[m^3/h]$

$\boldsymbol{D}$: Pipe Diameter [m]

$\boldsymbol{g}$: Gravitational Acceleration $[m/s^2]$

$\boldsymbol{\rho}$: Density of Water $[kg/m^3]$

$\boldsymbol{h}$: Head Conversion Factor $[-]$

$\boldsymbol{q}$: Flow Conversion Factor $[-]$

$\boldsymbol{n_q}$: Specific speed $[-]$

$\boldsymbol{N}$: Rotation speed of PAT $[rpm]$

$\boldsymbol{\phi}$: Flow Coefficient [-]

$\boldsymbol{\varphi}$: Head Coefficient [-]

$\boldsymbol{\lambda}$: Power Coefficient [-]

$\boldsymbol{P}$: Power $[W]$

SUBSCRIPTS

site : Site Characteristic

T : Turbine mode

P : Pump mode

Upstream : Upstream

Downstream : Downstream

Bypass : Bypass

eff : Effective

ABBREVIATIONS

PAT : Pump as Turbine

PRV : Pressure Reducing Valve

WDN : Water Distribution Network

ANN : Artificial Neural Network

CFD : Computational Fluid Dynamic

LIST OF FIGURES

LIST OF TABLES

1 INTRODUCTION

Energy is the cornerstone of humankind. We need to spend enough energy on all activities that act up in the world. As energy production is not enough according to the growing population in developing countries, it plays an important role for them to save or produce more efficiently. From the past till up to nowadays, electricity generation is common from non-renewable sources. One of the most common types of non-renewable sources is thermal power plants. It burns coal, natural gas, petroleum, etc. to generate electricity. These fuels release harmful gasses to the environment such as CO_2, NO_x, CO, and CH_4. These gasses are Greenhouse gases (GHG). They trap some of the Earth's outgoing energy, thus retaining heat in the atmosphere. This heat-trapping causes changes in the radiative balance of the Earth (the balance between energy received from the sun and emitted from Earth) that alter climate and weather patterns at global and regional scales. Also, other problems that these released gasses consequence can be listed as acid rains and toxic wastes. These problems are associated with the use of non-renewable energy sources. All of these problems push us to use more environmentally friendly, greener, more efficient energy production solutions.

There are a lot of renewable energy sources and can be listed as wind power, solar energy, biomass, geothermal energy, hydropower energy, tide energy, and wave energy. Among all of these sources, hydropower is the most promising and often used to produce electricity. Small and micro-hydropower projects are excellent alternatives for electricity generation in remote areas. Small scale hydropower projects can be installed on small streams, small rivers, and canals without any recognizable effect on the environment. As compared to large-scale hydro projects, small-scale hydro projects can be installed in less time and with a low initial cost without any extensive environmental problems. Small and micro-hydropower projects are the appropriate options for generating electricity by using such water streams. The running cost of such plants is low but the initial capital cost is relatively high. So, reducing the equipment cost in small hydropower projects can become more useful and accessible. One of the easiest ways to reduce the equipment cost is the use of a centrifugal pump in reverse (turbine) mode which can be used as an alternative to conventional hydraulic turbines.

Pump as turbines stand out with its easy applicability and environmental friendliness in micro hydroelectric power generation. PATs have different scales and applications as mentioned above literature review. Among these applications, the subject of interest in recent years has been the use of PATs in the water distribution networks of cities. Pressure reducing valves used in WDNs are used to reduce pressure on water going to cities or small towns to prevent any damage or explosion in pipelines. PRVs cannot generate electricity, but if we use PAT instead of PRVs, we can generate electricity and reduce the pressure on the outgoing water. Thus, we recover the mechanical energy losses in PRVs.

1.1. Applications of PAT

There are several applications of PAT in energy recovery applications. However, the hydropower plants that are over 100 kW require large space and they pollute the environment usually. A journal article shows that in large hydropower plants micro-hydro energy recycling systems will be in demand due to the space shortage and environmental damage factors [1] Then A.A. Williams discussed the advantages of using PAT in micro-hydropower plants. He said compared to turbines, pumps have a large head, flow rate, number and size can be found, and the parts of the pump are much more accessible in the sector without being expensive. [2]

B. Teuteberg finished report in 2010. [3] This report covered the design process of a micro-hydro development at Roman Bay Sea Farm in Gansbaai. In this farm, B. Teuteberg investigated the financial and technical requirements of the 97 kW micro-hydropower plants with PAT. He found out that the project's viability depends on the electric tariff of the region. He saw the viability of the project If sufficient conditions supplied the project.

K. Motwani, S. Jain, and R. Patel ran a case study. In this study, a 3-kW capacity Pico hydro test rig was developed by installing the PAT, and the maximum overall efficiency of the PAT was found to be around 60. It is lower than the Francis turbine, which is around 80 percent. But in the Pico hydro range, the cost of a Francis turbine can be 6 to 8 times more than that of a centrifugal pump. For the economic rationale of PAT, an annual life cycle cost analysis is done as a case study. According to the analysis, the annual life cycle cost (ALCC) was found to be 6.8 and 5.07 per unit cost of electricity produced between Francis's turbine and PAT, respectively, which justified the

use of PAT instead of Francis turbine for the case under study. PAT application is recommended at the point of maximum efficiency in Pico/micro-hydro. [4]

Although micro-hydro power plants, PATs can be used in WDNs instead of PRVs for energy recovery application. Bryan Orchard reported that energy recycling can be achieved by using pumps as turbines in the water industry. At the same time, the use of pumps in such facilities is much easier and less costly than turbines in 2009. [5]

Pressure control is an essential component of the safe operation of water supply systems. In general, PRVs are used to maintain standard pressures in areas with high system topology and topography. PRVs dissipate all the energy present in the fluid through heat loss. A turbine can be used instead of PRVs to generate electrical energy and control pressure. Exactly at this point, using PATs instead of PRVs will reduce the investment cost. However, due to dynamic operations during the day, PATs must operate under varying flow and pressure conditions. This change affects efficiency head loss. This complicates the selection of PATs to replace PRVs with conventional methods.

According to a report shared in the 73rd Conference of the Italian Thermal Machines Engineering Association [6] a MATLAB® Simulink model is developed for simulating a branch of the WDN located in Laives (South-Tyrol). To run PAT at their best efficiency point (BEP) a speed control by means of an inverter is performed due to the high variability of the flow rate inside the grid branch. In results, where the flow rate is nearly constant, the energy produced does not offset the capital cost of electrical equipment for rotational speed control. Considering the average daily flow rate and head, a pump named Calpeda N32/125 is selected with a method that correlates the specific speed, specific diameter, and efficiency of PATs in turbine mode (N_{ST}, D_{ST}, η_t) with the ones in pump mode (N_{SP}, D_{SP}, η_P) for a branch that simulated in MATLAB®. Simulation shows that when the PAT's speed is controlled, the energy recovery rate increases by about 23%. Also, that would lead to a significant decrease in the payback period (PBP).

In 2020, Michele Stefanizzi and others [7] shared a report. In this report, The WDN of a town in the Apulia region (Southern Italy) has been used as a case study. The report proposes a methodology to select a PAT for a specific WDN. The methodology gives a chance to evaluate the required specific speed by the site and also when the PAT's geometrical information is known PAT characteristic curve can be predicted by using 1D performance prediction. While selecting

PAT the average daily flow rate and corresponding head were selected for turbine BEP operating conditions ($Q_{BEP,\,T}$ and $H_{BEP,\,T}$). Then the corresponding BEP's parameters ($Q_{BEP,\,P,}$ and $H_{BEP.P}$) are predicted. In this case, NSC 150-400/900 was selected by using Xylem®. In this case study, PAT used two different ways to control the PAT's efficiency and pressure drop of WDN. One is installing PAT with series PRV which means hydraulically controlled. The second is installing rotational speed control. As a result, the second case increases energy production by an amount of 4.5% researchers neglected the second because economically it is not worth it. In general, research shows that using PAT in WDN in this case study has a 24-month payback period.

[8] In this study, researchers tried to optimize a PAT set-up for specific WDN conditions. They constructed three scenarios to analyze the wide range of PAT. To select part PSO technique is used. In the first scenario, the operating speed of the PATs is the same and constant during a day. In the second scenario operating speeds are different for each PAT but constant during a day. In these two scenarios when the network consumption is high PAT's energy recovery performance and pressure reduction performance are good. However, when the network consumption is low both performances dropdown. In the last scenario, PAT's operating speed is variable. As a result, the energy consumption slightly decreases but the total pressure reduction performance is significantly increased except at the start and end hours of the day. To obtain continued pressure reduction performance researchers suggest that the PAT and PRV are installed serially, this system can work dynamically throughout the day so that pressure reduction and energy recovery are obtained.

1.2. Selection of PAT

[9]This study shows the characteristics of the PAT at various rotational speeds by comparing the respective flows and heads of a centrifugal pump used as a turbine. In this way, it is possible to observe the effect of rotational speed on efficiency, as well as obtain the characteristics at constant pressure and leakage speed. In addition, using computational fluid dynamic (CFD) analysis, the forces acting on the impeller were also examined. The research results show that the turbine characteristics can be predicted to some extent from the pump characteristics, that the water flows through the impeller without a whirlpool at the best efficiency point, and that the radial stresses are lower than in the pump mode.

[10] Xu Tan and Abraham Engeda tried to predict accurate turbine mod operation characteristics of the centrifugal PAT. The proposed method is most accurate because it is based on both specific speed and the specific diameter of PAT. In this work, four centrifugal pumps are used for analysis. The method uses curve fitting of the specific speeds, specific diameters, and efficiency ratios in turbine mode and pumps mode. As a result, the specific speed correlation is approximately linear. The specific diameter correlation tends to be linear. However large errors in head and flow prediction. On the other hand, since efficiency ratio prediction is related to specific speed prediction, it is roughly linear (less than 5% error). However, the geometrical difference of the pumps deflected the predictions. Because of that more tests are needed for different pump designs.

[11]In this paper, M. Rossi and M. Renzi tried to develop a correlation between PAT's pump mode parameter and turbine mode parameters. To do that non-dimensional analysis, coupled with the normalization process was performed. Three coefficients are used in the dimensionless analysis: flow coefficient (ϕ), head coefficient (ψ), and power coefficient (Λ). The coefficients are evaluated taking into account the flow rate m^3/h, the head $[m]$, the power output of the PAT $[W]$, the impeller diameter $[m]$ and the revolution $\left[\frac{rad}{sec}\right]$ different PATs in literature are analyzed. As a result, different geometries deflected the correlation.

[12]In this work, researchers proposed a methodology for selecting the correct PAT for a specific site. Statistical models and one-dimensional code are used for this method. Researchers defined the conversion factors C_Q (Capacities ratio between turbine mode and pump mode at BEP), C_H (Heads ratio between turbine mode and pump mode at BEP) to be able to find the required capacity and flow rate of the pump for the chosen site.

[13]In this study, an experimental investigation of performance prediction of PAT. The study proposed a more robust model to predict PAT's performance. The experiments firstly are done on the single-stage centrifugal pump. While constructing the characteristic curve of the PAT the BEP specific speed model is selected instead of the BEP efficiency model because of its accuracy. The results show that the prediction error is ± 10%.

[14]In this paper, M. Renzi and M. Rossi are continuing their previous study. They used 32+27 BEP experimental tests available in the literature. Moreover, a new method was proposed for the prediction of hydraulic efficiency (η) at BEP. With non-dimensional analysis hydraulic efficiency

of turbine mode at BEP (η_t) formalized as a function of the specific speed of the pump (N_{Sp}) and hydraulic efficiency of the pump (η_p). he proposed methodology led to better results in terms of ψ, η, Λ and N_S evaluation, while slightly worse results are obtained in terms of both Φ and D_S evaluation if compared to other models.

[15]In this article, variable speed PAT has been used as SPRS (Soft Pressure Regulating System) technology in combination with a variable frequency drive that controls PAT by changing the torque on the generator continuously. It causes changes in rotational speed and consequently, the operating point of PAT varies up to be matched with available head and flow. Also, it regulates the frequency of generated power that is injected into the grid to remain constant at 50 Hz. PAT operation should meet the desired pressure control that is reducing the pressure to the expected values. PAT performance prediction is divided into two steps: BEP prediction and entire curve estimation. Available models that specify BEP of PAT compared with the results and mean conversion factor errors for flow and head reported as 7.33% and 23.83%, respectively. For estimating the off-design operation of PAT, experimental data were plotted in non-dimensional curves, and it was found that employing rotational speed in the modeling relationships would improve the prediction results. Finally, the specific speed of the pump should be considered in using mathematical predictive models because pumps with much lower or higher specific speeds might not operate similarly, also the range of flow number values can limit the functional area of the relations.

1.3. CFD Analysis of Pat

[16]The 3D geometry of the horizontal single suction volute type centrifugal pump was selected to analyze the characteristics of the PAT. The model pump was meshed by ANSYS ICEM-CFX based on finite volume methods (FVM). Under the non-cavitation condition, the impeller domain was rotating on the y-axis at 1750 RPM with different flow operating conditions, and the suction pipe and volute were on a stationary domain. A frozen rotor was applied to couple the rotation and stationary domains. All boundary walls were assumed to be smooth walls with non-slip conditions. The SST turbulence model was used to solve the turbulence phenomena of the fluid. High resolution for the advection scheme, the first order for the turbulence numeric and SIMPLEC

algorithms were considered in the solver control. The residual value was $1x10^{-5}$ controlled by convergence criteria.

For cavitation analysis, the flow conditions were considered a steady-state, incompressible, homogeneous two-phase flow (water and vapor). The saturated vapor pressure was set at 3169 Pa. The Reynolds-averaged Navier-Stokes (RANS) equations with the SST turbulence model were discretized by the FVM and Rayleigh-Plesset cavitation model was adopted. Advection terms dealt with high-resolution discretization schemes. The residual for velocity and pressure was set to $1x10^{-5}$ as convergence criteria.

To confirm the numerical results, simulation results were validated with experimental data. A good agreement between the two results was obtained at given flow rates. In this comparison, the average deviation of the head values was only 3.01%, the highest deviation of 12.67% for the highest flow rate at 1750 rpm. The pump efficiency shows an average deviation was only 3.63% and the highest deviation was 8.53% for the highest flow rate of $559.68\ \frac{m^3}{hr}$. Also, for the pump shaft power, the average deviation was only 4.74%.

The pump head decreases with the increasing flow, but the head consumed by the turbine increases with the increasing flow rate. Efficiency was 85.67% at the rated flow rate of $450\frac{m^3}{h}$ at pump mode but in the turbine mode, the flow rate of $368.64\ \frac{m^3}{h}$ the maximum efficiency was 76.90%. The efficiency difference was only 9.96%. The power output was 34.47 kW at pump mode and the power output was only 41.76 kW at turbine mode. In this case, the power increased up to 4.3% than pump mode.

On the other hand, the velocity contours were observed in the flow field of the PAT mode at a flow rate of $450\frac{m^3}{h}$. The velocity was smoothly distributed at the pump mode and high velocity occurred at the volute chamber near the corner. But in the turbine mode, the velocity is unevenly distributed. The velocity was low at the leading edge of the impeller and flows were separated due to the wake of formation. This phenomenon occurs because of the relative velocity drop at the impeller inlet (turbine mode) resulting from the recirculation zone.

The initial decrease of the cavitation did not affect the head drop line because the pump and the total head remained unchanged. When cavitation number decreases, total head decreases and drops

sharply at lower σ. This head drop varies for different flow rates. When the flow rates are larger than Q_{dp} ($Q > Q_{dp}$) heads are smaller than the Q_{dp} ($Q < Q_{dp}$), heads are larger than that of it. From these results, 3% head drop accounted for cavitation conditions. It is seen from the literature that the predicted head drop shows a similar trend with experimental results.

At turbine mode, the cavitation effects are similar to those of the pump mode. Cavity volume fraction variation with different σ, i.e., 0.178, 0.143, 0.11, and 0.092 at the design flow rate $450\frac{m^3}{h}$ at pump mode. The cavitation occurrences were observed in the developed pump impeller. The cavitation bubbles grew and appeared at first on the suction zone near the blade leading edge. The pressure in this section was smaller than the shroud due to the centrifugal force of the pump impeller. When the σ value decreases, the cavitation region increases from leading suction edge to trail edge, which was a significant factor on the impeller blades. For $\sigma = 0.110$, at that point, the pump head began to drop. In this case, the pressure loading was increased on the impeller blade. For $\sigma = 0.092$, the cavitation length was almost fully formed on the blade impeller and the length of bubble cavities increased from the leading edge to the trailing edge.

Also, cavitation performances were investigated in the turbine mode at a flow rate of 368.64 $\frac{m^3}{h}$. The volume fraction of water vapor distribution on the runner blades at four different Thoma cavitation numbers ($\sigma = 0.876$, $\sigma = 0.743$, $\sigma = 0.801$, and $\sigma = 0.782$) at rated condition. It is seen from the figures that as the cavitation number decreases more vapor bubbles are generated near the leading edge on the blade suction side. Vortex cavitation occurred on the impeller hub centrally in turbine mode.

In comparison, in the pump mode, the cavitation first occurred at the suction leading edge on the impeller blades and attached cavitation observed on the impeller blade at the lower suction head; however, for the turbine mode, the development of vortex cavitation happened at the impeller hub centrally and outlet near the trailing edge on the impeller blades.

At pump mode, at a rated flow rate of $450\frac{m^3}{h}$ the maximum efficiency was 85.67%. But in the turbine mode, the maximum efficiency was 76.90% at the flow rate of 368.64 $\frac{m^3}{h}$. The power output was 37.47 kW at pump mode, but power output was only 41.76 kW at turbine mode. The use of an existing pump as a turbine is applicable. The turbine mode efficiency of 77% was

relatively lower than the pump efficiency of 85%. Nevertheless, the turbine efficiency is not bad to use as a turbine. When turbine mode was adopted, cavitation performances were estimated and described according to different σ. Results of the current work show that vortex cavitation can directly lead to losses in efficiency.

2 MATERIALS AND METHODS

2.1. Pump Selection Methodology

As mentioned in the literature review (1.2.Selection of), the flow conditions of the region where the application will be made are the most important factors in this regard. Fortunately, research in recent years has found various and effective model to solve this problem. The common goal was to create models that could estimate the turbine mode's Best Efficiency Point (BEP) based on the pump mode's BEP, which could be found in catalogs. The conversion factors for the parameters at both BEPs are expressed in terms of head convergence factor, h, and flow conversion factor, q, as stated in (2-1) and (2-2).

$$h = \frac{H_{BEP,T}}{H_{BEP,P}} \tag{2-1}$$

$$q = \frac{Q_{BEP,T}}{Q_{BEP,P}} \tag{2-2}$$

Used pump selection methodology in this project can be seen in the flow chart (see **Figure 2-4**). This methodology is one of the newest and most basic and adapted from M. Stefanizzi [7]. According to methodology, in order to obtain maximum effectiveness turbine mode flow characteristics $H_{BEP,T}$, $H_{BEP,T}$ should be equated to the region flow characteristics, H_{site}, Q_{site}. Also, one step ahead the specific speed of turbine mode $n_{q,T}$ can be calculated with knowing rotational speed of the pump N as stated in equation (2-3).

At this point, by using empirical correlations which proposed by M. Stefanizzi the pump BEP

$$n_{q,T} = N \frac{\sqrt{Q_{BEP,T}}}{\sqrt[4]{H_{BEP,T}{}^3}} \tag{2-3}$$

prediction model is constructed. These empirical correlations reported in **Figure 2-1**, **Figure 2-2** and stated as in equations (2-4),(2-5).

$$n_{q,P} = \frac{\left(n_{q,T} + 2.6588\right)}{0.9237} \tag{2-4}$$

$$h = (-3x10^{-5}){n_{q,T}}^3 + (0.0043){n_{q,T}}^2 - (0.1938)n_{q,T} + (3.4671) \tag{2-5}$$

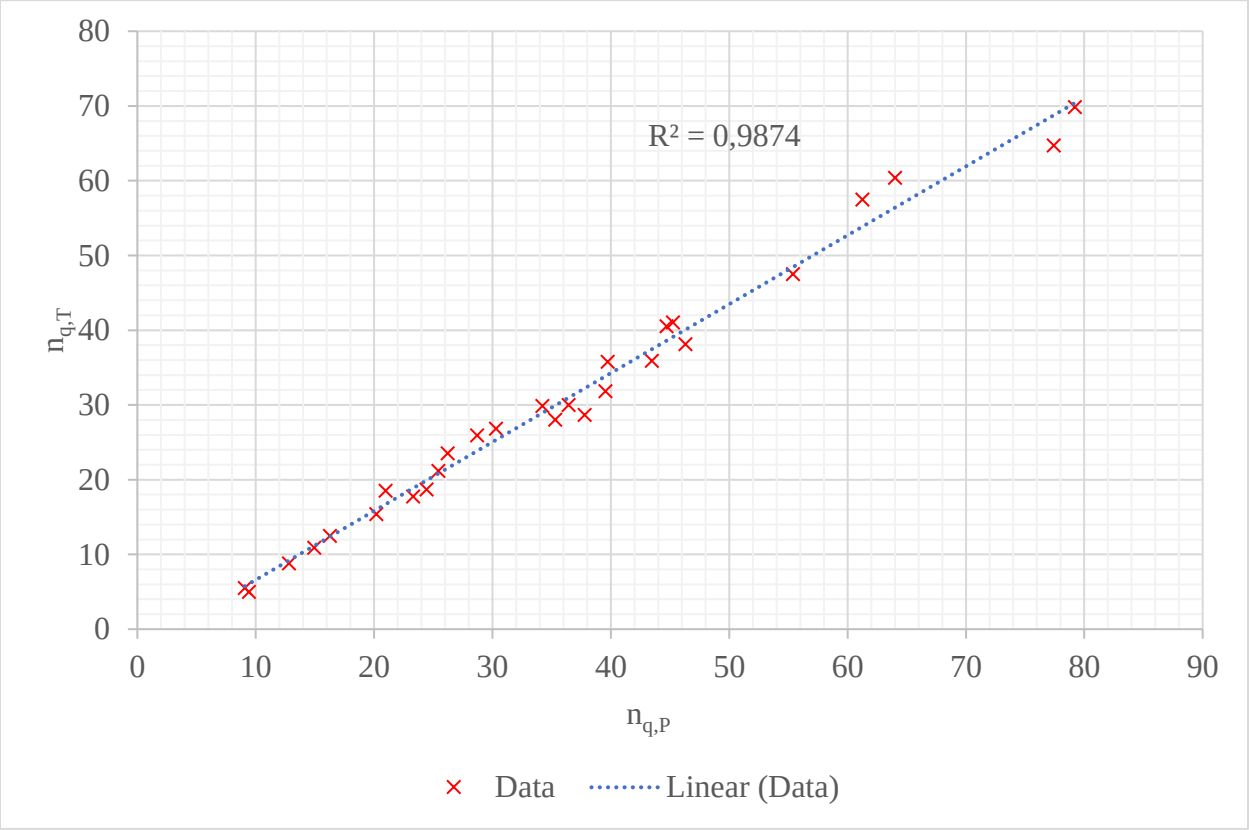

Figure 2-1: Specific speed number in turbine mode, $n_{q,T}$, vs. specific speed number in pump mode, $n_{q,P}$.

With this data the BEP characteristics of the pump mode can be computed by using definition of flow coefficient (See equation (2-1)) and specific speed (See equation (2-3)) of the pump mode as reported in equation (2-6),(2-7).

$$H_{BEP,P} = \frac{H_{BEP,T}}{h} \tag{2-6}$$

$$Q_{BEP,P} = \left(\frac{n_{q,P} {H_{BEP,T}}^{0.75}}{N}\right)^2 \tag{2-7}$$

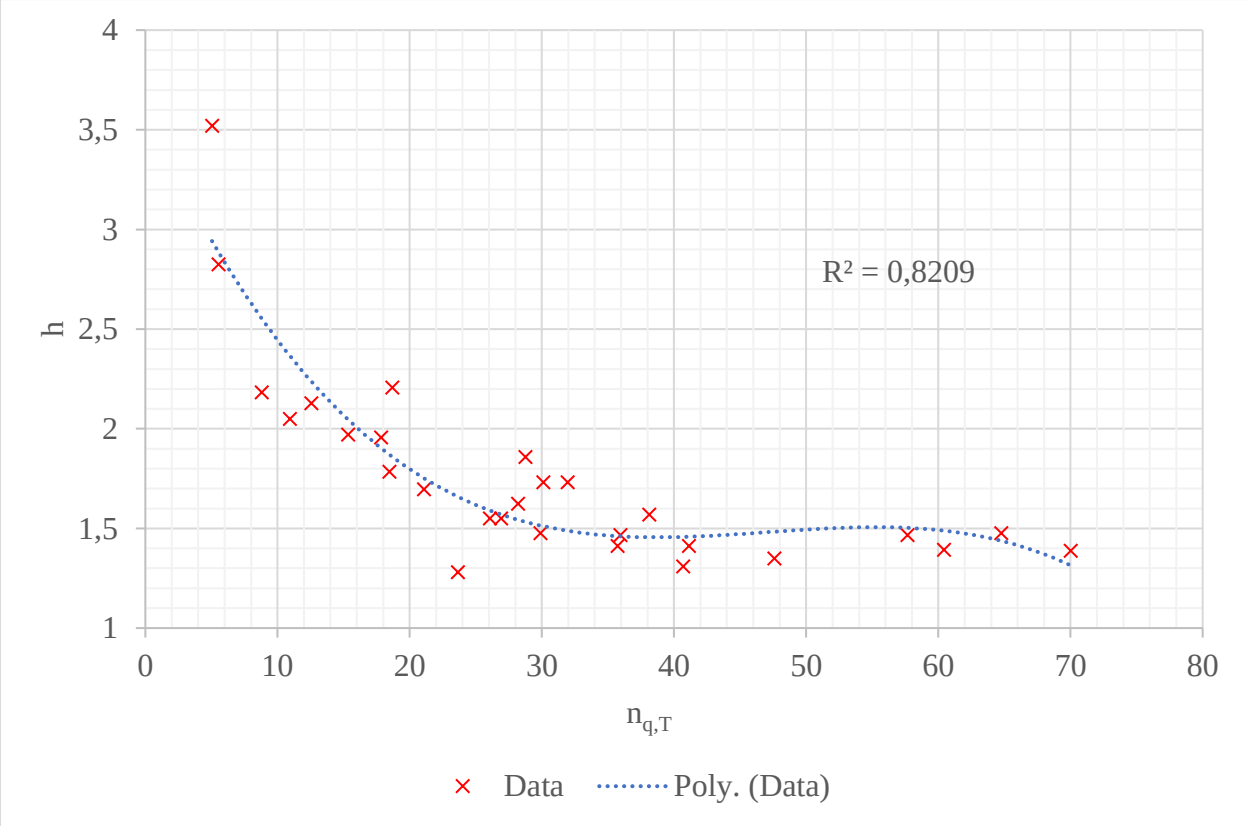

Figure 2-2: Empirical correlation that obtained by plot digitizer [19] Head ratio, h, vs. specific speed number in turbine mode, $n_{q,T}$.

It is necessary to notifyee that, output of the model depends on the method and sample machines that used to obtain data. However, as long as the speed range isn't too wide, the approach can

produce reliable projections. Therefore, in this model is used specific speed number which collects main performance parameter of the machine.

As a result, with knowing $Q_{BEP,P}$, $H_{BEP,P}$, $n_{q,P}$ the desired pump can be selected from catalogues. Indeed, the theoretical part of the methodology is completed at this point. Furthermore, it can be possible to predict PAT performance curve by using 1D prediction method which is constructed considering detailed geometrical measurement of machine. These properties are only available from pump manufacturers. There are some works that proposed this model [20].

2.2. Working principle of PAT System

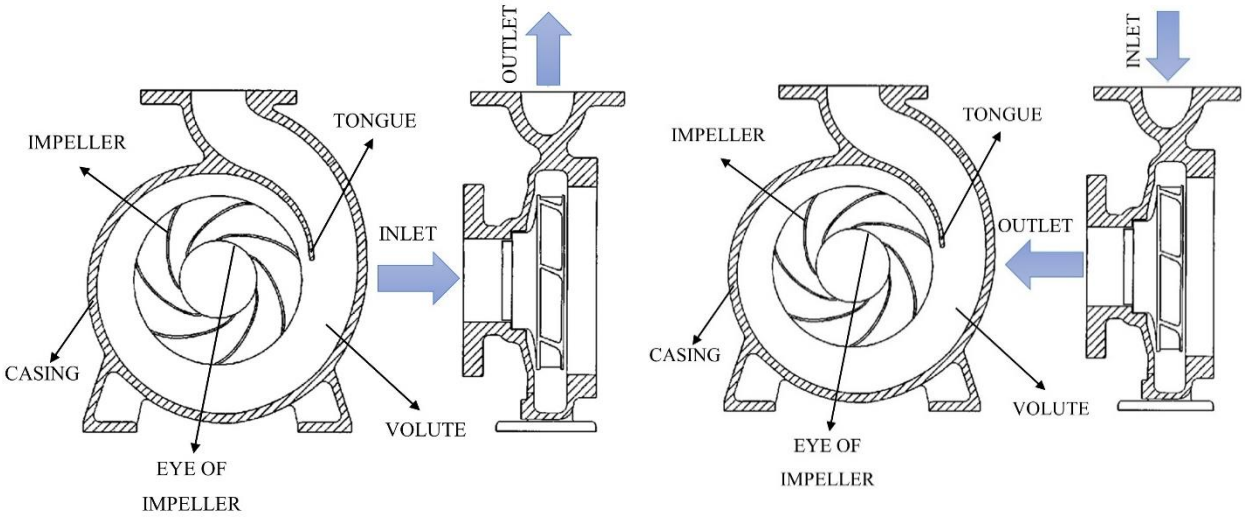

Figure 2-3: Pump mode (a), PAT mode (b).

Before explaining working principle of the PAT, first, pumps' working principle should be understood. A pump has impeller, casing, electric motor, casing, shaft, bearing etc. components and some of them can be seen in the **Figure 2-4(a)**. When electrical energy supplied to the motor, rotor starts rotating around its axis, and all of the produced torque is transmitted through to the impeller with the help of shaft. Impeller has blades on its surface that is specifically designed to change water's pressure. At the inlet of the pump, pressure of the water is lower rather than its outlet. So, it increases pressure at the outlet. If we reverse this process by forcing water through the outlet of the pump, we get our PAT. This time, at the inlet of the PAT (see **Figure 2-4(b)**), if we force high pressure water to pass, it rotates the impeller without using any electricity and leaves

the PAT at the outlet. The rotating impeller transmits torque to the motor with the help of shaft and produces electrical energy.

2.3. Curve Prediction Method

This method is obtained by using empirical correlation which created with Artificial Neural Network by M. Rossi [14]. According to this method, dimensionless factors that are flow coefficient (ϕ), head coefficient (φ) and power coefficient (λ) are constructed as in equations (2-8),(2-9), and (2-10).

$$\phi = \frac{Q\left[\frac{m^3}{s}\right]}{N\left[\frac{rad}{s}\right](D[m])^3} \tag{2-8}$$

$$\varphi = \frac{g\left[\frac{m}{s^2}\right]H[m]}{\left(N\left[\frac{rad}{s}\right]\right)^2(D[m])^2} \tag{2-9}$$

$$\lambda = \frac{P[W]}{\rho[\frac{kg}{m^3}]\left(N\left[\frac{rad}{s}\right]\right)^3(D[m])^5} \tag{2-10}$$

At this point, since the characteristic curves of the pump mode are known. The turbine mode's best efficiency point data $\phi_{BEP,T}$, $\varphi_{BEP,T}$, and $\eta_{BEP,T}$ can be obtained by using empirical correlations (see equations (2-11), (2-12), (2-13)) with inputs of pump mode's best efficiency point data $\phi_{BEP,P}$, $\varphi_{BEP,P}$, and $\eta_{BEP,P}$. These correlations are obtained from literature by using plot digitizer. (See Appendix A:)

$$\phi_{BEP,T} = (0.97077)\phi_{BEP,P} + 0.00698 \tag{2-11}$$

$$\varphi_{BEP,T} = (2.47108)\varphi_{BEP,P} - 0.09297 \tag{2-12}$$

$$\eta_{BEP,T} = (0.77443)\eta_{BEP,P} + 0.1264 \tag{2-13}$$

Then by combining results of the above equation and correlation that the obtained from ANN, the flow versus head and flow versus efficiency curve can be obtained via equations (2-14), (2-15), and (2-16).

$$\frac{\varphi_T}{\varphi_{BEP,T}} = (0.2673)\left(\frac{\phi_T}{\phi_{BEP,T}}\right)^2 + (0.7330)\left(\frac{\phi_T}{\phi_{BEP,T}}\right) \tag{2-14}$$

$$\frac{\lambda_T}{\lambda_{BEP,T}} = (1.589)\left(\frac{\phi_T}{\phi_{BEP,T}}\right)^2 + (0.6193)\left(\frac{\phi_T}{\phi_{BEP,T}}\right) \tag{2-15}$$

$$\begin{aligned}\frac{\eta_T}{\eta_{BEP,T}} = &-(0.0787)\left(\frac{\lambda_T}{\lambda_{BEP,T}}\right)^6 + (0.8540)\left(\frac{\lambda_T}{\lambda_{BEP,T}}\right)^5 \\ &-(3.6005)\left(\frac{\lambda_T}{\lambda_{BEP,T}}\right)^4 + (7.4998)\left(\frac{\lambda_T}{\lambda_{BEP,T}}\right)^3 \\ &-(8.1546)\left(\frac{\lambda_T}{\lambda_{BEP,T}}\right)^2 + (4.4475)\left(\frac{\lambda_T}{\lambda_{BEP,T}}\right)\end{aligned} \tag{2-16}$$

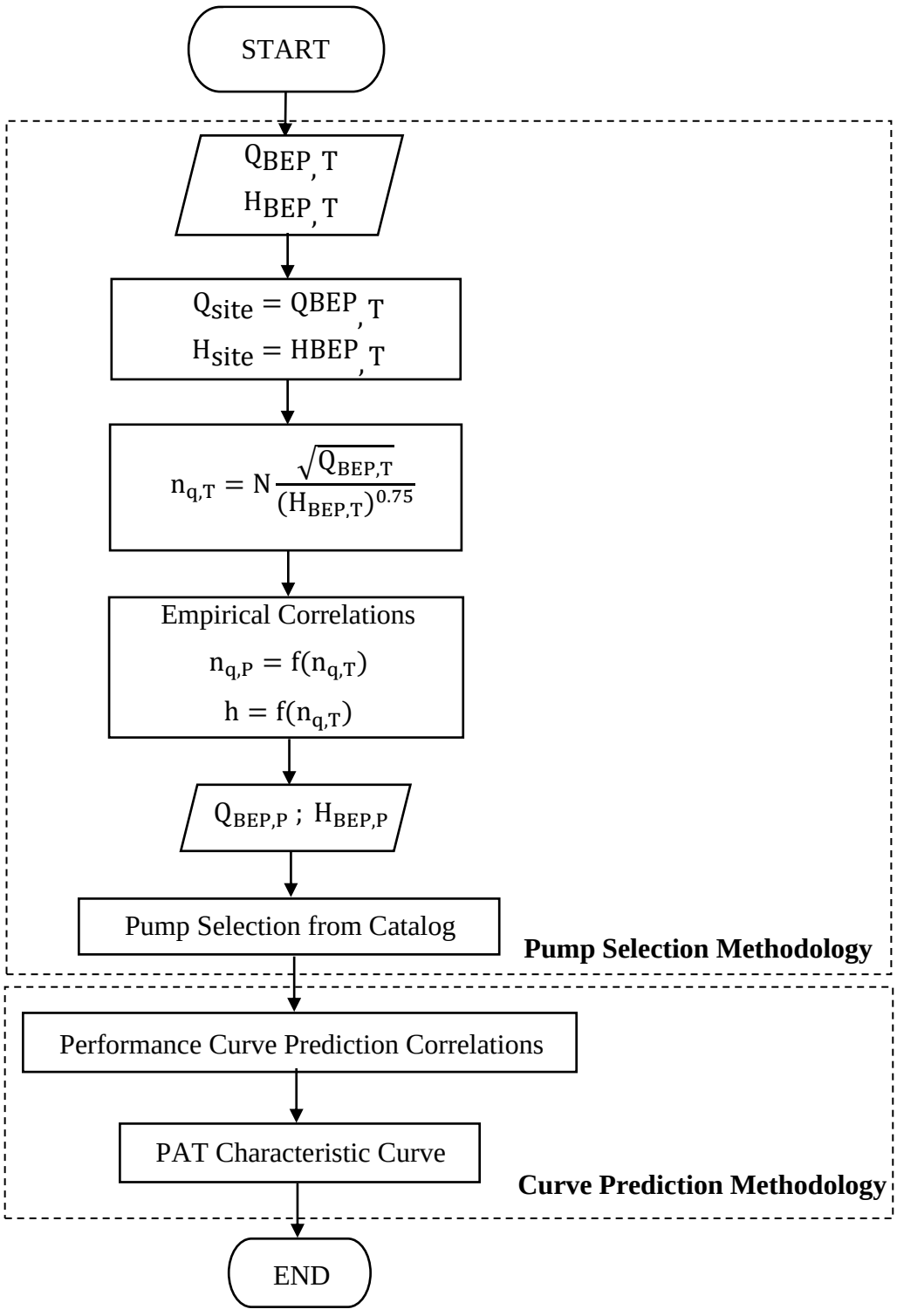

Figure 2-4: Flow chart of project.

3 CASE STUDY

In this project to validate and obtain economic analysis of the PAT system. Moreover, organizational insufficiency and permission requirements. Case study condition is adapted from literature [21]. The adapted flow regime of the WDN is reported in **Figure 3-1**, **Figure 3-2**. In these data, daytime is defined as 05.00 to 16.00 and nighttime is 16.00 to 05.00.

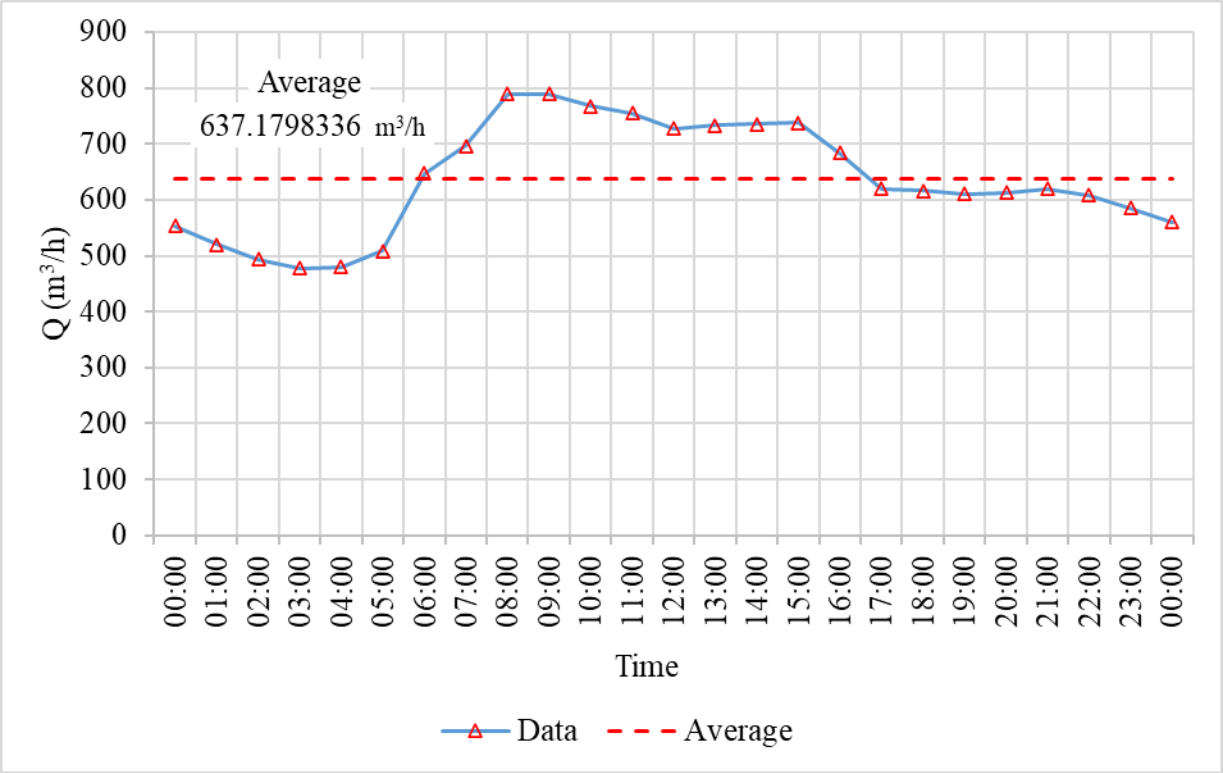

Figure 3-1: Adapted flow regime data of WDN.

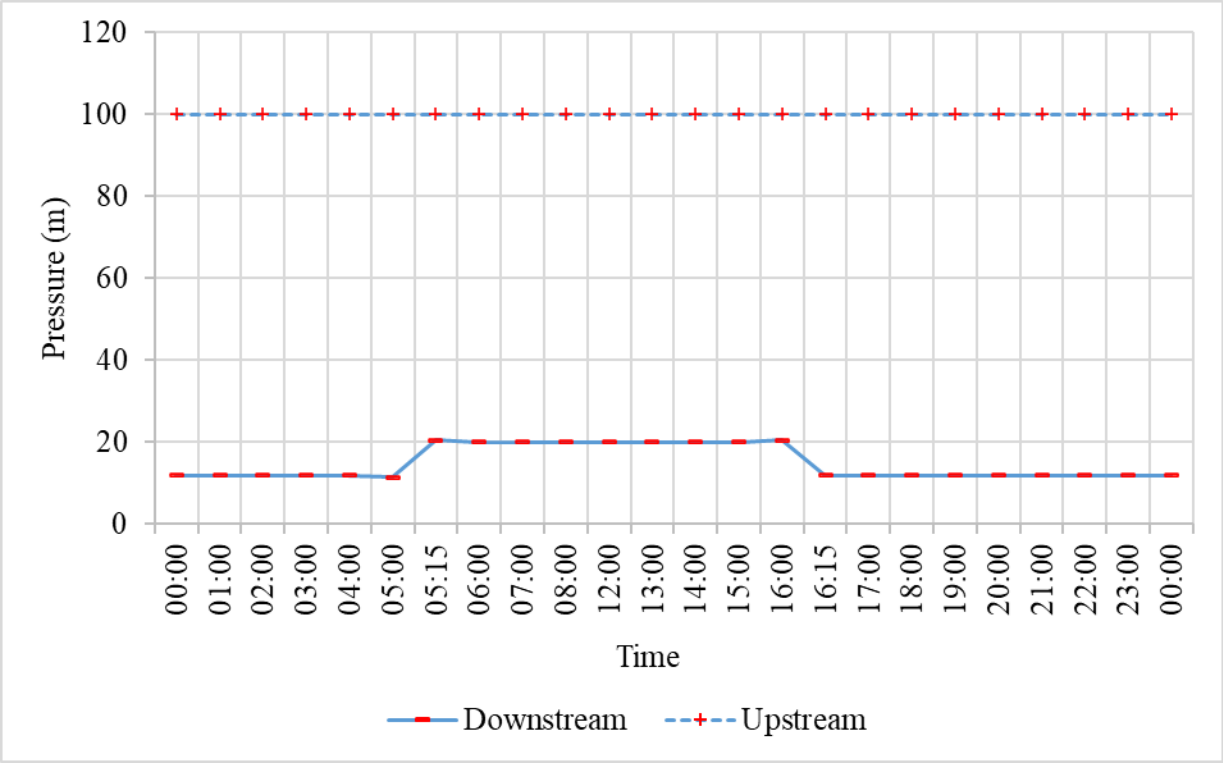

Figure 3-2: Adapted Pressure gradient of WDN.

From the average flow rate data in the **Figure 3-1**, and according to the methodology (see **Figure 2-4**), $Q_{BEP,P}$, and $H_{BEP,P}$ calculated as 434.8 $\frac{m^3}{h}$, and 48.461 m respectively by using MATLAB®. Thus, these results enabled us to select a suitable centrifugal pump from the catalogue. The pump brand is KSB, model is Etanorm 200-150-400 [22]. Pump has an efficiency of 86.2% on the pump mode and has an impeller diameter of 405 mm. Performance and Efficiency-Flow Rate curves are given in **Figure 3-3**, and **Figure 3-4**.

From the efficiency and performance data of the pump and using the prediction method (See 2.1.Pump Selection Methodology), PAT's best efficiency point, efficiency curve, and performance curve can be estimated. Performance, and Efficiency-Flow Rate curves are given in the **Figure 3-5**, and **Figure 3-6**.

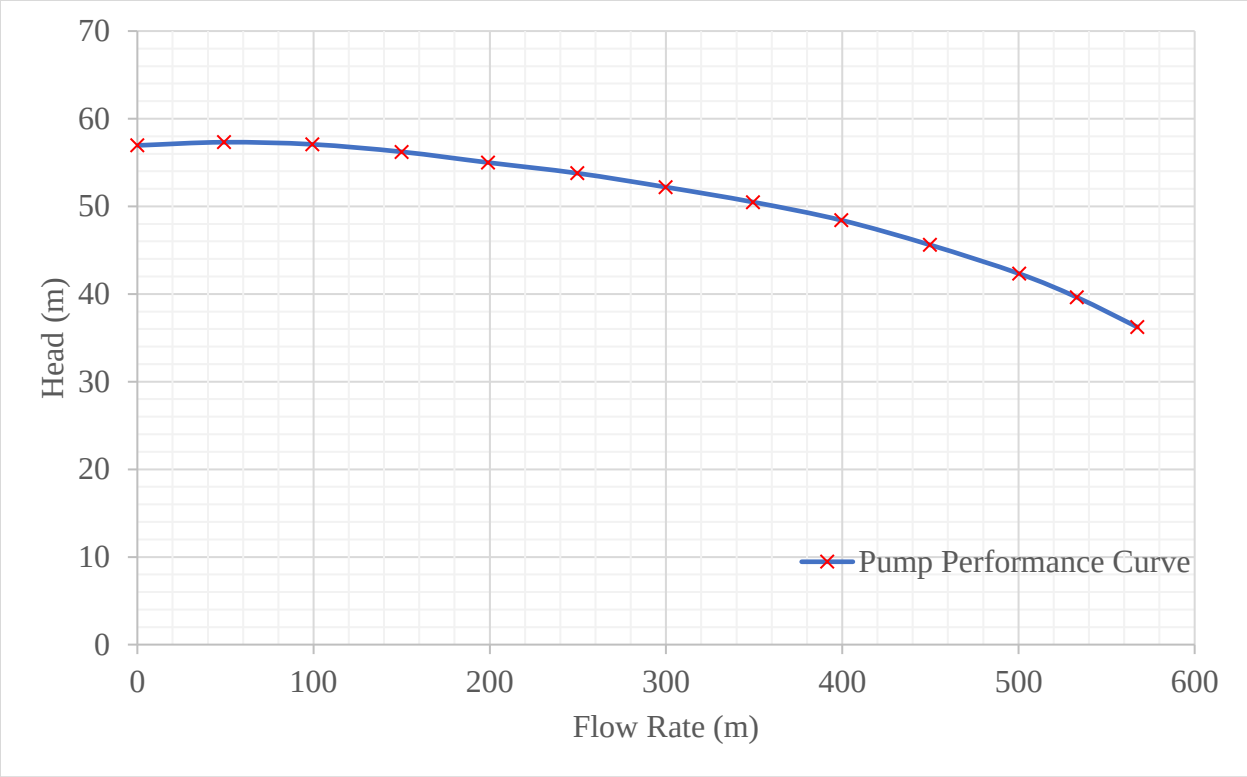

Figure 3-3: Performance curve of the KSB Etanorm 200-150-400.

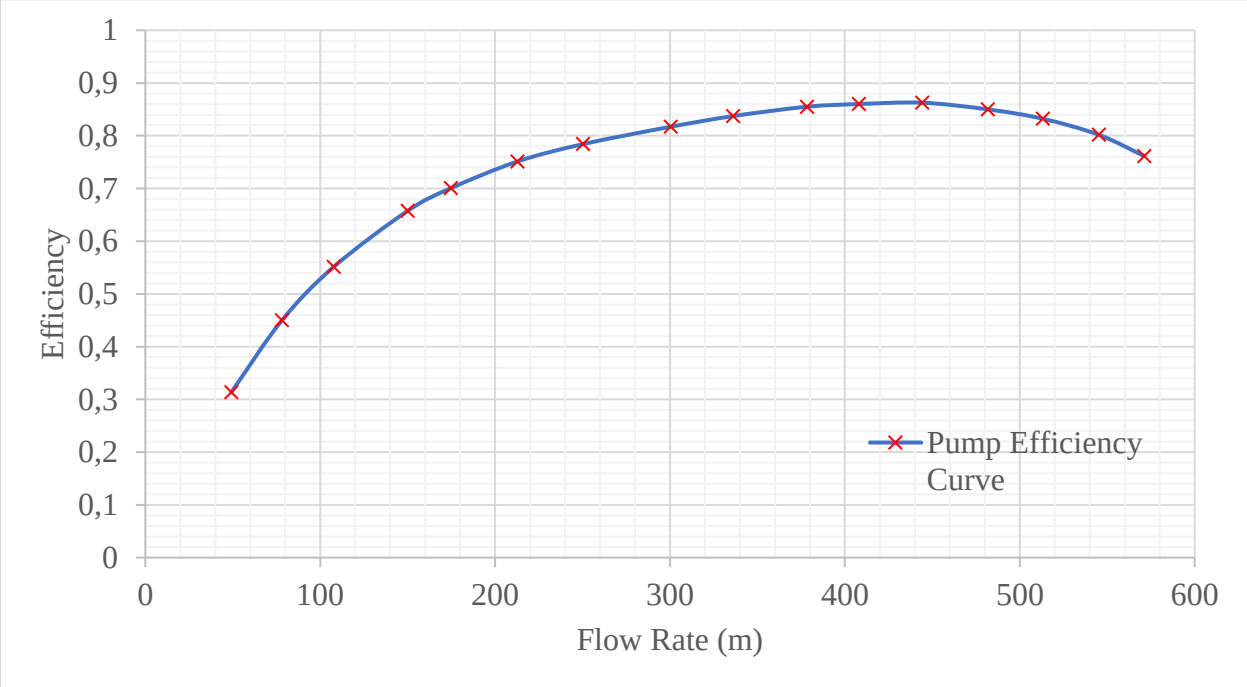

Figure 3-4: Efficiency-Flow Rate curve of the KSB Etanorm 200-150-400.

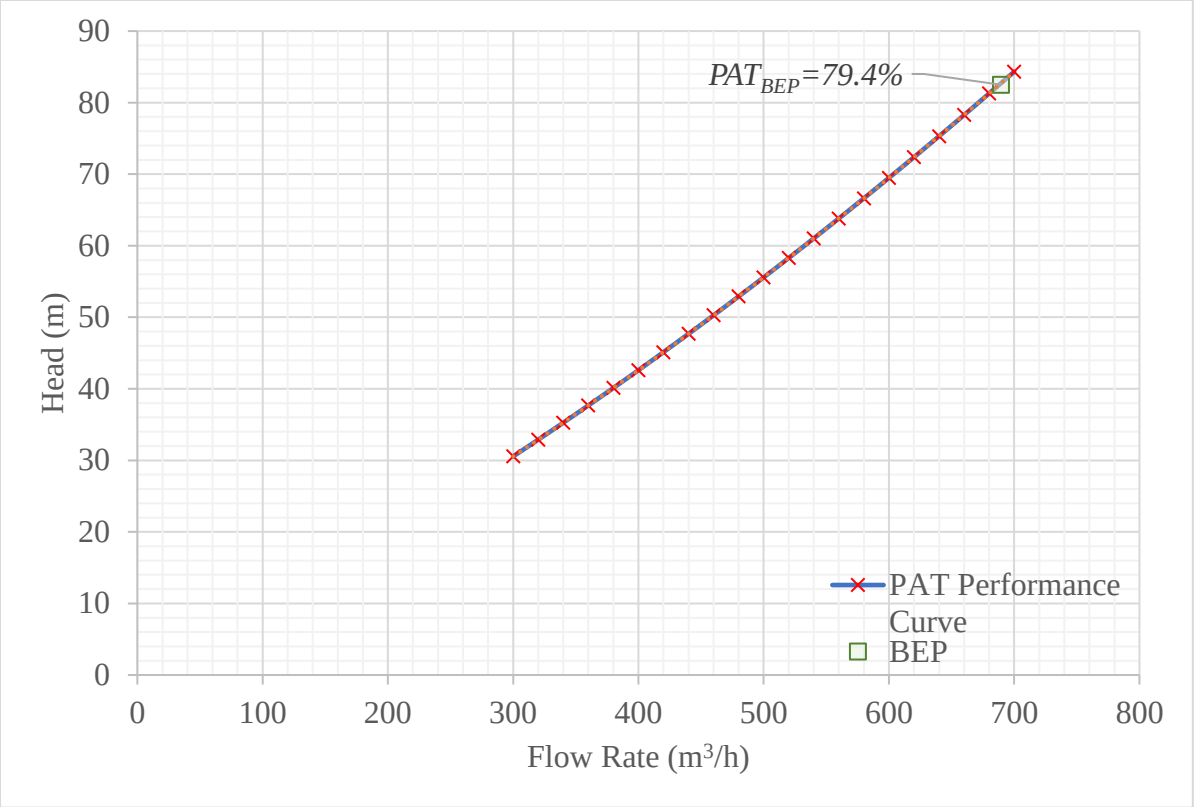

Figure 3-5: Performance curve of the PAT.

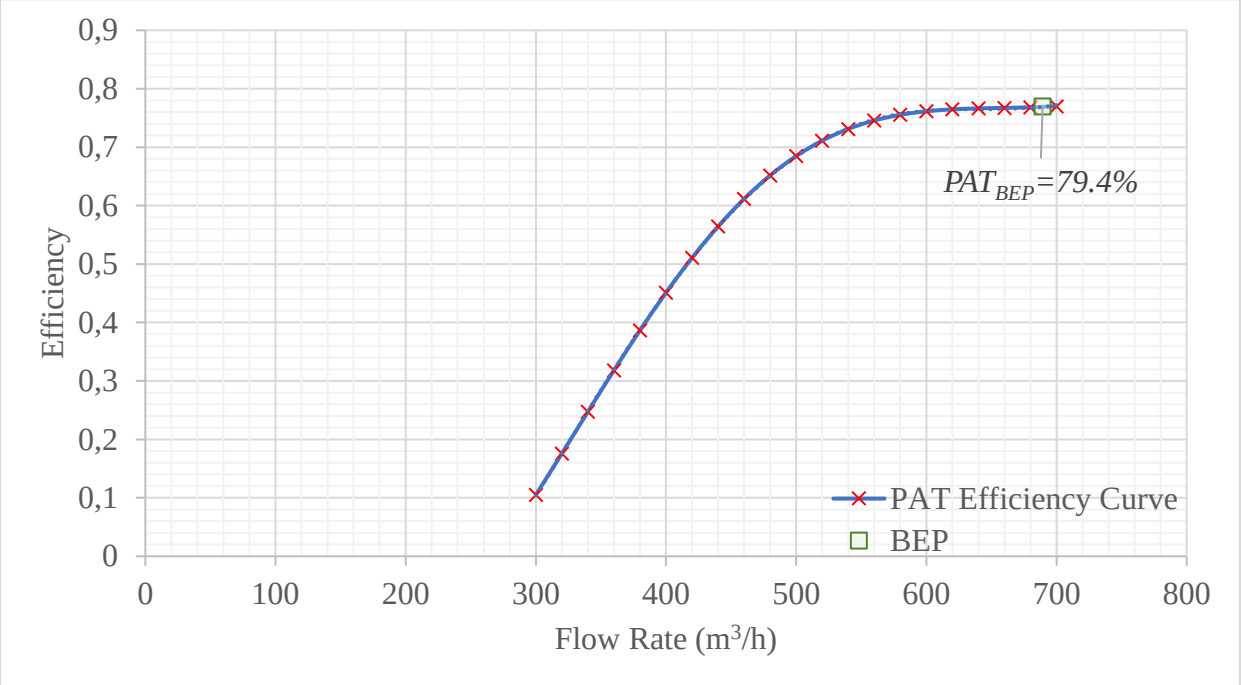

Figure 3-6: Efficiency-Flow Rate curve of the PAT.

As mentioned in the earlier sections, meeting the desired pressure drop is as important as generating energy during the PAT application, because it is one of the two factors that determine the feasibility of the project.

The system design put forward as a solution to above problem in the literature (See Figure 3-7) [21]. In this system, water flow from the tank is expressed as $Q_{Upstream} = 637.18\ \frac{m^3}{h}$, and the water flow to the town is expressed as $Q_{Downstream}$. If the $Q_{Upstream}$ coming to the PAT system is higher than the $Q = Q_{BEP,T} = 678.04\ \frac{m^3}{h}$, PRV #1 is left on full capacity and $Q_{Upstream}$ is bypassed with the help of PRV #2. In this case, upstream water flow can be stated as in equation (3-1). Thus, PAT is protected from efficiency reduction caused by possible overload, and lifespan of the PAT will be increase.

If the Upstream flow to the PAT system is lower than $Q_{BEP,T}$, PRV #2 is closed completely, and the $Q = Q_{Upstream}$ coming to PRV#1 is regulated and transferred to the PAT according to the needs. At the end of both cases, the flow coming from PAT and PRV #2 is regulated in the Main PRV for to maintain desired pressure drop and sent to the town as $Q_{Downstream}$. So, Main PRV is used as an emergency system in the case of any fail situation for PAT.

$$Q_{Upstream} = Q_{BEP,T} + Q_{Bypass} \tag{3-1}$$

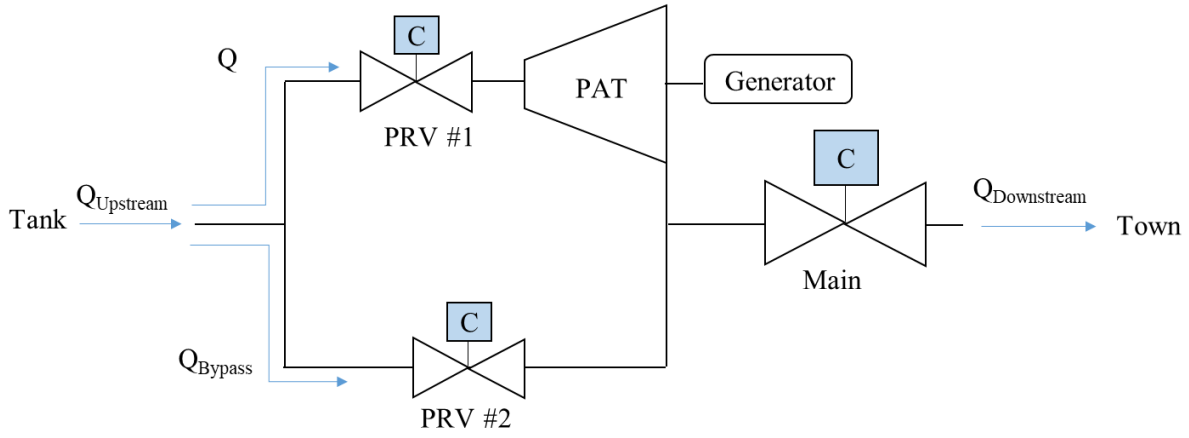

Figure 3-7: Schematic installation of PAT system.

After the theoretical calculations, and system design (See Figure 3-8), entire day, PAT produces 2290.15 kW electricity power. At the daytime, PAT produces an average of 109.05 kW of electricity power but, due to low usage of water at town, and subsequently the low flow regime at nighttime, average electricity power production reduces to 75.50 kW. Detailed daily available energy in WDN and produced energy by PAT is reported in Table 3-1. Between 07:00 and 15:00, normally, flow is changing between 695 $\frac{m^3}{h}$, and 788 $\frac{m^3}{h}$, but to protect pump, and to increase efficiency of the PAT, PRVs are used as seen in the Figure 3-7**.**

Table 3-1: Daily data of produced and available energy.

Available Energy [kWh/day]		
Night time	Day time	Total
1,910.41	1,752.24	3,662.64
Energy Production by PAT [kWh/day]		
Night time	Day time	Total
978.13	1,306.47	2,284.59

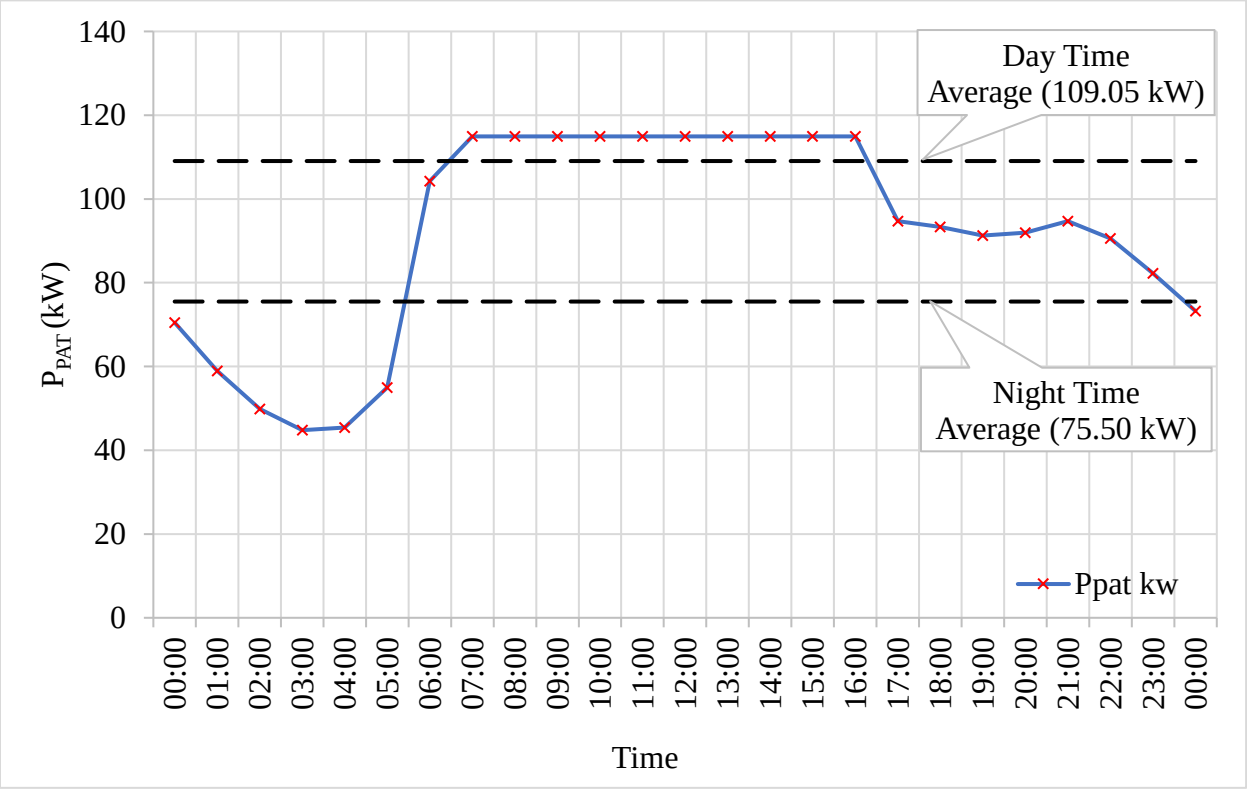

Figure 3-8: Effective power that is produced by the PAT.

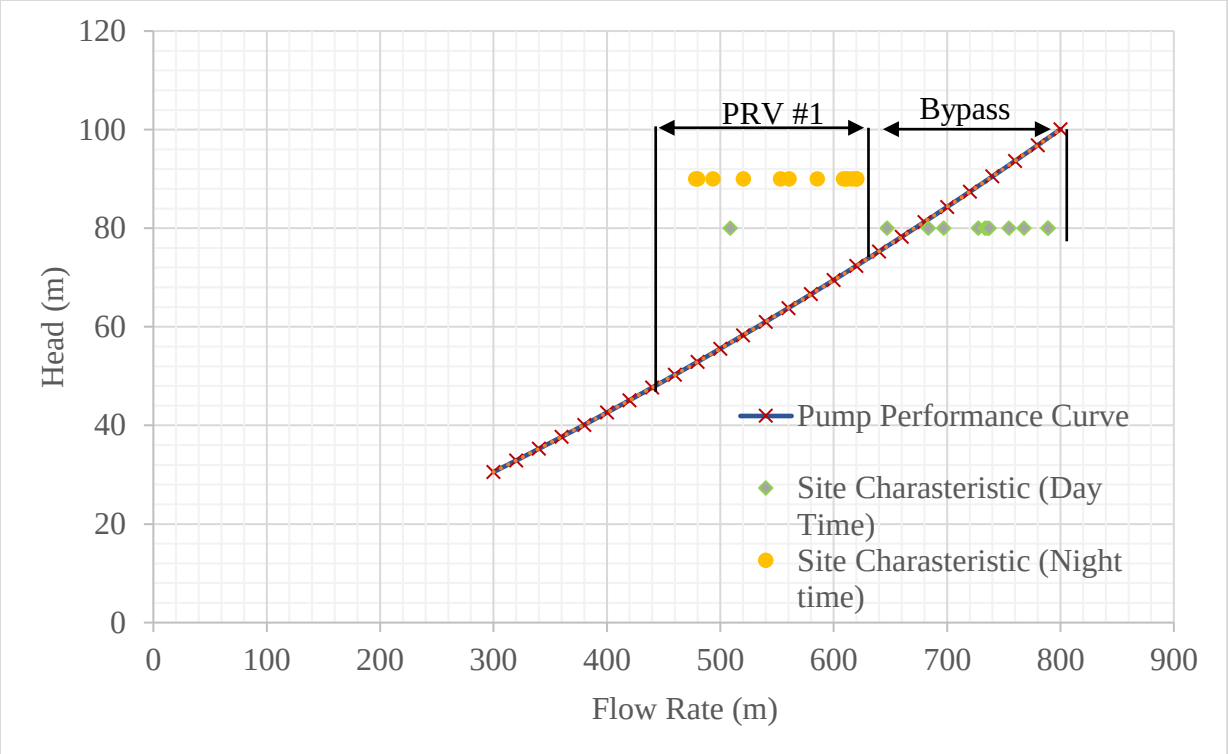

Figure 3-9: Predicted PAT performance curve with site characteristic

4 RESULTS AND DISCUSSION

According to constructed methodology, when the flow regime and head characteristic of a specific site are known, user can select a PAT. Further, user can analyze the PAT performance with this method whether its beneficial or not without any experimental procedure. If the accuracy of the methods used is to be discussed, pump selection methodology consists of two empirical correlations (See Equations (2-4),(2-5)) and curve prediction methodology consists of six empirical correlations (See Equations (2-11),(2-12),(2-13), and (2-14),(2-15),(2-16)). In the **Table 4-1** all correlation's R^2 values are reported. Values are taken from literature. Furthermore, the overall R^2 value of methodology can be calculated as 0.803.

Table 4-1: Correlation's R^2 values with experimental data and average R^2 value.

Equation	R^2
(2-4)	0.821
(2-5)	0.987
(2-11)	0.894
(2-11)(2-12)	0.401
(2-11)(2-13)	0.490
(2-14)	0.913
(2-15)	0.974
(2-16)	0.946
Average	0.803

4.1. CO_2 Emission

The financial benefits of energy produced by PAT are reported in the **Table 4-2**. In Turkey, produced electric can be sell 2.063 TL/kWh [23] . On the other hand, this system generates the energy from the mechanical energy of water, which would normally be any loss. Since no fossil fuels or chemicals are used during this process, it does not emit CO_2, which is the most damaging to the world. In this case, the average amount of CO_2 emissions corresponding to the energy produced can be calculated. According to report released in 2021 for kWh electrical energy, 0.0004-ton CO_2 emitted to atmosphere. Also, in Turkey each ton of CO_2 is 2720 ₺ [24].

Table 4-2: Produced Energy and Value of Produced Energy

Parameter	Per Unit Value	Total Value
Annual Produced Energy [$kWh/year$]		833876.39
Value of Produced Energy [₺]	2.063 [₺/kWh]	1671025.89
CO_2 reduction [$ton/year$]	0.0004 [ton/kWh]	333.55
Value of Reduced CO_2 in Turkey [₺]	2720 [$ton/$₺]	907257.51

Moreover, the CO2 emissions of motor vehicles were used to better understand the environmental benefit of the clean energy produced by the PAT system. In the **Table 4-3**, the average distance traveled by a car in Istanbul [25] and the amount of CO_2 emitted per kilometer by a car in Istanbul

[26] can be seen. All data in the table consist of mean values. According to the table, it can be said that the PAT system prevents the CO_2 emissions of 195 car in Istanbul annually.

Table 4-3: Environmental Benefit of PAT with respect to the car in Istanbul.

Parameter	Value
Average Distance of a Car in Turkey $[km]$	14,236.00
Average CO2 Emission rate of a Car in Turkey $[g/km]$	120.00
Average Annual CO2 Emission of a Car in Turkey $[ton]$	1.71
Number of Car that equal to the CO2 Emission Reduction of PAT	195

4.2. Cost Analysis

In order to calculate the detailed cost of the PAT system, it was necessary to contact companies that provide two main needs, such as the pump manufacturer and the manufacturer of electromechanical control systems. Within the scope of this project and in line with the possibilities at hand, excluding PAT and motor hydraulic equipment (PRV, measurement devices, pipes and fitting and labor cost), electronic equipment (SCADA system, electronic acquisition system, connection and cables), civil work and engineering cost are taken from literature. ([27] - [7] - [28]) The PAT and motor selected required motor power from the supplier web site [22]. The total cost of the PAT system is reported in **Table 4-4.** The maintenance cost is taken 2.5% of total capital cost per year [29]. It is average maintenance cost of the micro hydro power plants.

Table 4-4: Total cost of PAT system.

Expenses	Cost [₺]
PAT (with motor)	646,039.62
Hydraulic Equipment	3,271,680.00
Electronic Equipment	189,000.00
Engineering	310,410.00
Civil Work	524,700.00
Total Capital Cost	4,941,829.62
Maintenance Cost Per Year	123,545.74

In order to understand PAT system is good investment or not the payback period is reported in the **Table 4-5.** Fortunately, as discussed before sections PAT system has environmental benefits and these benefits can be turned into the economic value as seen in the **Table 4-2.** Hence, the value should be added to the payback period. As seen in the table below, PAT system creates significant environmental value.

Table 4-5: Economical payback period of PAT system.

Indicator	Value
Total Cost of the PAT System [₺]	4,936,699.62
Payback Period [year]	2.95
Payback Period Including Environmental Benefit [year]	1.91

5 CONCLUSION AND FUTUREWORK

In this study, a PAT system is intended to place before a WDN considering a real case study in literature. A pump named ETANORM 200-150-400 is selected by predicting pump mode's BEP characteristics from site characteristics. Used BEP prediction method is based on specific speed number (n_q). Reason of that it is combining the main performance parameter of the machine. Afterward, PAT performance curves are predicted from pump performance curves by using six correlations in literature. These correlations are obtained by using several ANNs. Since used correlations are taken from literature by using plot digitizer or directly, the plot digitizer's percentage error is tested and reported as ±1.28% maximum percentage error, ±0.292% average percentage error. Furthermore, as discussed previous section overall coefficient of determination of methodology is 0.803 which is quite high according to literature.

In the continuation, the economic analysis of the PAT system constructed in case study is performed. Considering proposed system in case study, daily energy production of plant is 2,284.59 kWh, annual energy production is calculated as 833,876.39 kWh. The value of this amount of energy in Turkey is computed and combined with cost analysis of the PAT system as a result total payback period of plant is almost 36 months. Considered cost analysis generally taken from literature except the PAT and motor. The reason of that is lack of contact with required companies. As mentioned previously, environmental benefits of PAT have been revealed, too. Since PAT doesn't emit any CO_2 during process, the amount of CO_2 reduction of plant is 333.55

ton. This amount of reduction is equal to the annual CO_2 emissions of 195 cars in Turkey. On the other When the economic value of the environmental benefit (CO_2 emission) of PAT computed, the annual value of the reduced CO_2 in Turkey is computed as 907,257.51 TL. If this value added to the annual return of PAT, the payback period is reduced to almost 24 months.

As a future work recommendation, any CFD analysis has been done within the scope of this project. Detailed CFD analyzes and real-time experiments can be performed to validate the formulas used in the methodology.

6 REFERENCES

[1] F. Manzano Aguigliaro, M.Taher, A. Zapata Sierra, A. Juaidi and F. G. Montoya, "An overview of research and energy evolution for small hydropower in Europe," *Renewable and Sustainable Energy Reviews,* vol. 75, pp. 476-489, 2017.

[2] Williams, A.A., "Pumps as Turbines for Low Cost Micro Hydro Power," *Renewable Energy*, vol. 9, no. 1-4, pp. 1227-1234, 1996.

[3] Teuteberg, B., "Design of a pump-as-turbine for an abalone farm Final report for mechanical project," *Research Gate,* 2010.

[4] Karan Motwani, Sanjay Jain and Rajesh Patel, "Cost analysis of pump as turbine for pico hydropower plants-a case study," *procedia,* pp. 721-726, 2013.

[5] Orchard. B., Klos. S., "Pumps as Turbines for water industry," *Elsevier,* vol. 2009, no. 8, pp. 22-23, 2009.

[6] Jacopo C. Alberizzia, Massimilian Renzia, Alessandra Nigroa, Mosè Rossi, "Study of a Pump-as-Turbine (PaT) speed control for a Water Distribution Network (WDN) in South-Tyrol subjected to high variable water flow rates," in *73rd Conference of the Italian Thermal Machines Engineering Association*, Pisa, Italy, 12-14 September 2018.

[7] Michele Stefanizzia, Tommaso Capursoa,Gabriella Balaccob,Mario Binettib, Sergio Mario Camporealea, MarcoTorresia, "Selection, control and techno-economic feasibility of Pumps as Turbines in Water Distribution Networks," *Elsevier,* vol. 162, no. Renewable Energy, pp. 1292-1306, 2020.

[8] Kandi, Shahin Ebrahimi Alireza Riasi Ali, "Selection optimization of variable speed pump as turbine (PAT) for energy recovery and pressure management," science direct, 9 November 2020.

[9] Fernandez. J., Blanco. E., Parrondo. J., Stickland. M., Scanlon. T, "Performance of a Centrifugal Pump Running in Inverse Mode," Journal of Power and Energy I MechE., 2004.

[10] Xu Tan, Abraham Engeda, "Performance of centrifugal pumps running in reverse as turbine: Part II- systematic specific speed and specific diameter based performance prediction," *Elsevier,* vol. 99, no. Renewable Energy, pp. 188-197, 2016.

[11] Renzi, M. Rossi and M., "Analytical Prediction Models for Evaluating Pumps as Turbines (PaTs) Performance," *Elsevier,* vol. 118, pp. 238-242, 2017.

[12] S. Barbarelli, M. Amelio, G. Florio and N. M. Scornaienchi, "Procedure Selecting Pumps Running as Turbines in Micro Hydro Plants," *Energy Procedia,* vol. 126, pp. 549-556, 2017.

[13] M. Stefanizzia, M. Torresia, B. Fortunatoa, S.M. Camporealea, "Experimental investigation and performance prediction modeling of a single stage centrifugal pump operating as turbine," 72nd Conference of the Italian Thermal Machines Engineering Association, Lecce, Italy, September 2017.

[14] Massimiliano Renzi, Mosè Rossi , "A general methodology for performance prediction of pumps-as-turbines using Artificial Neural Networks," *Energy Procedia,* vol. 158, pp. 117-122, 2019.

[15] Mojtaba Tahani, Ali Kandi, Mahdi Moghimi, Shahram Derakhshan Houreh, "Rotational speed variation assessment of centrifugal pump-as-turbine as an energy utilization device under water distribution network condition," *Energy*, vol. 213, pp. 118-502, 2020.

[16] Md Rakibuzzaman, Keum-Young Jung, and Sang-Ho Suh,, "A Study on the use of Existing Pump as Turbine," 2019.

[17] pOrbital, "Plot Digitizer," pOrbital, [Online]. Available: https://plotdigitizer.com/. [Accessed 10 05 2022].

[18] Tommaso Capurso, Marco Torresi , Giuseppe Pascazio ,Sergio Ranaldo ,Michele Stefanizzi, Sergio M. Camporeale , Bernardo Fortunato and Rosario Monteriso, "Development of a 1-D Performance Prediction Model," proceedings, Bari, Italy, 2018.

[19] Michele Stefanizzia, Tommaso Capursoa,Gabriella Balaccob,Mario Binettib, Sergio Mario Camporealea, MarcoTorresia, "Selection, control and techno-economic feasibility of Pumps as Turbines in Water Distribution Networks," 26 August 2020.

[20] "ksb.com," KSB, [Online]. Available: https://www.ksb.com/en-fr/lc/products/pump/dry-installed-pump/etanorm/E04B. [Accessed 11 06 2022].

[21] "epdk," epdk, [Online]. Available: https://www.epdk.gov.tr/Detay/Icerik/3-1327/elektrik-faturalarina-esas-tarife-tablolari. [Accessed 11 06 2022].

[22] I. E. Agency, "Turkey energy Policy Review," 2021.

[23] TUİK, "data.tuik.gov.tr," 2019. [Online]. Available: https://data.tuik.gov.tr/Bulten/Index?p=Tasit-kilometre-Istatistikleri-2019-37409. [Accessed 11 06 2022].

[24] Murat Şenzeybek and Peter Mock, "PASSENGER CAR EMISSIONS IN TURKEY," *WHITE PAPER*, p. 12, 2019.

[25] Mosè Rossia, Alessandra Nigroa, Giuseppe Roberto Pisaturoa, Massimiliano Renzia, "Technical and economic analysis of Pumps-as-Turbines (PaTs) used in an Italian Water Distribution Network (WDN) for electrical energy production," 10th International Conference on Applied Energy, ICAE, Hong Kong, China, 22-25 August 2018.

[26] Alessandro Morabito Patrick Hendrick, "Pump as turbine applied to micro energy storage and smart water grids: A case study," *Elsevier*, no. applied energy, p. 5478, 2019.

[27] "Inter National Renewable Energy Agency," irena, [Online]. Available: https://www.irena.org/costs/Power-Generation-Costs/Hydropower. [Accessed 11 06 2022].

7 APPENDIX

Appendix A: Curve Prediction Methodology Fitting Data

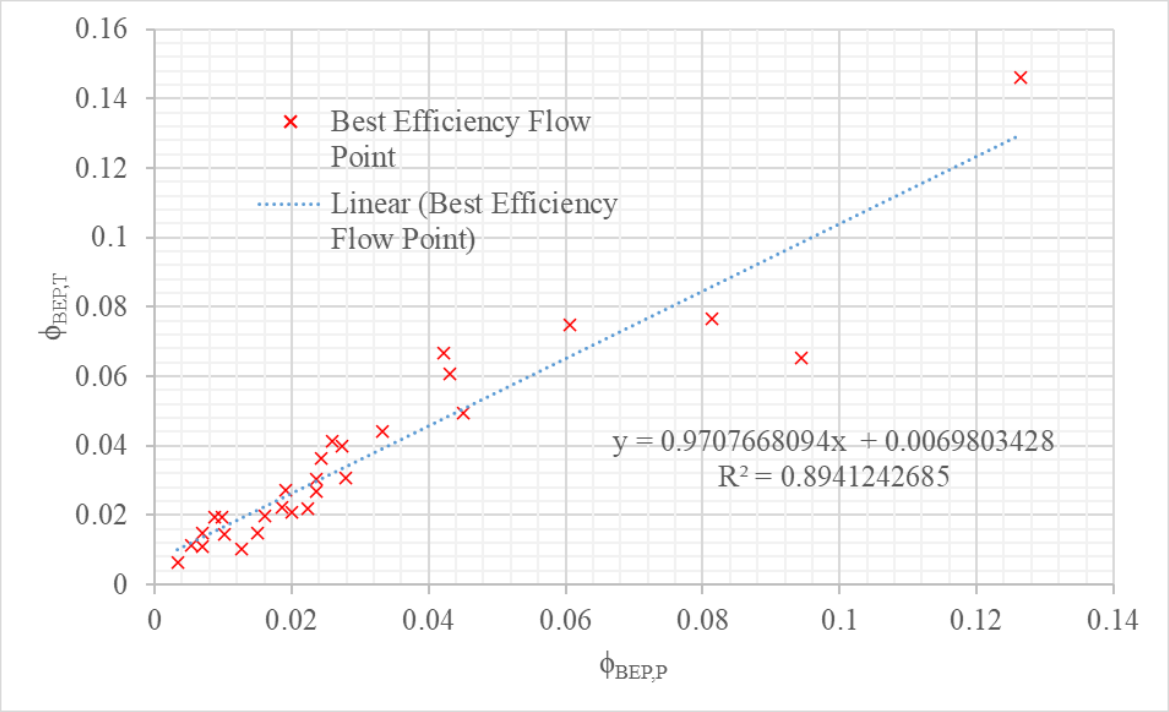

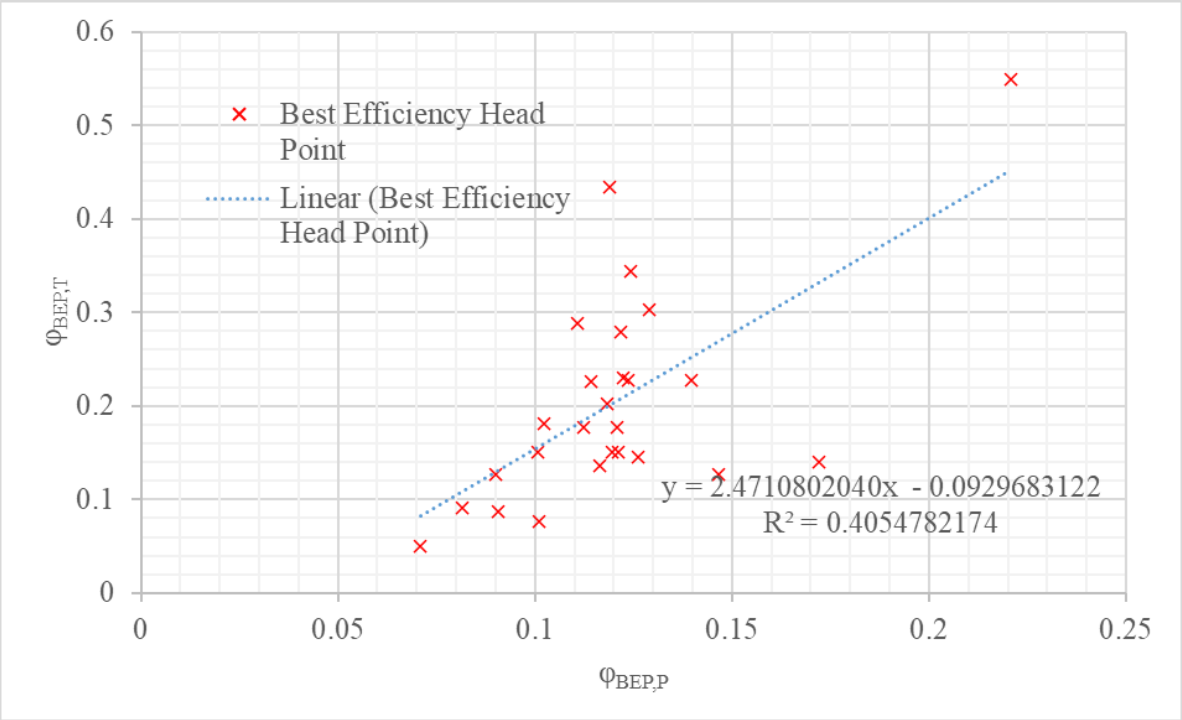
Best Efficiency Head Point
Linear (Best Efficiency Head Point)
y = 2.4710802040x - 0.0929683122
R² = 0.4054782174
φBEP,T
φBEP,P
0.6
0.5
0.4
0.3
0.2
0.1
0
0
0.05
0.1
0.15
0.2
0.25

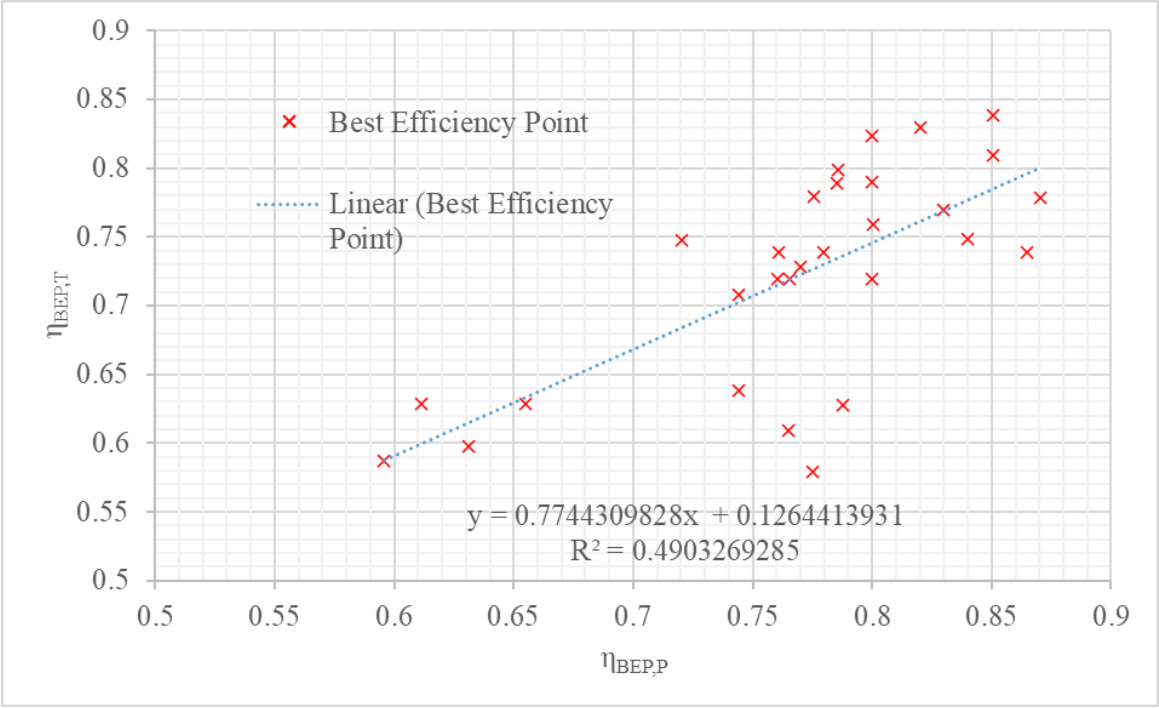
Best Efficiency Point
Linear (Best Efficiency Point)
y = 0.7744309828x + 0.1264413931
R² = 0.4903269285
ηBEP,T
ηBEP,P
0.9
0.85
0.8
0.75
0.7
0.65
0.6
0.55
0.5
0.5
0.55
0.6
0.65
0.7
0.75
0.8
0.85
0.9